CHEMISTRY
A EUROPEAN JOURNAL

DOI: 10.1002/chem.200500908

New Cyanine–Oligonucleotide Conjugates: Relationships between Chemical Structures and Properties

Rémy Lartia[a, b] and Ulysse Asseline*[a]

Abstract: Because the influence of the chemical structure of monomethine cyanine–oligo-2′-deoxyribonucleotide (ODN) conjugates on their binding and fluorescence properties has remained largely undetermined, we synthesized and studied a wide range of conjugates with various structural patterns. Different cyanine dyes such as thiocyanine, quinocyanine, and thiazole orange isomers were obtained. In the case of unsymmetrical cyanines, the linker was attached to either the quinoline or the benzothiazole nucleus. The influence of the ODN counterpart was evaluated by linking the cyanines to the 5′-end or to an internucleotidic phosphate. In the first case, the influence of neighboring nucleic bases was studied, whereas in the second, the stereochemical configuration at the phosphorus atom bearing the cyanine was investigated. We report here on relationships between the structures of the dyes and conjugates and some of their properties, such as the stability and fluorescence changes observed on their hybridization with the target sequence. This study provides useful information towards the design of ODN–cyanine conjugates.

Keywords: cyanines · dyes/pigments · fluorescent probes · oligonucleotides

Introduction

The completion of the Human Genome Project[1,2] has opened the way to greater progress in various areas such as the identification of genetic variants for applications in pharmacogenomics,[3,4] genetic causes of inherited and acquired diseases,[5,6] and gene organization and function analysis.[7,8] These studies require detection, with high sensitivity and excellent specificity, of sequences in different formats in vitro and in living cells. Most methods are based on base-pairing properties of nucleic acids. The detection of a specific target sequence in a complex nucleic acid mixture involves the hybridization of a labeled single-stranded oligonucleotide (ODN) probe. Hybridization assays can be performed on a solid phase or in homogeneous solution. The first method facilitates the separation of bound from unbound analytes but faces the problem of nonspecific adsorption,[9] steric hindrance on the microarray surface,[10] and nonspecific hybridization.[11] The second method requires the separation of hybridized and free probes, which is incompatible with experiments in living cells. The separation step can be eliminated by a probe whose signal changes on hybridization.[12,13] The most commonly used strategies in developing such probes include quenching/dequenching,[14,15] fluorescence resonance energy transfer,[16,17] luminescence resonance energy transfer,[18] and excimer formation.[19–23] Another strategy is based on modification of the signal generated by a single fluorescent or luminescent DNA binding agent linked to ODNs on hybridization with their target sequences. The minor-groove binder Hoechst 33258[24,25] and intercalating agents such as a ruthenium complex[26–28] have been covalently tethered to ODNs and fluorescent or luminescent (in the case of the ruthenium complex) signal increases were observed on hybridization of these labeled probes. Pyrene–ODN conjugates have also been successfully used to discriminate perfectly matched duplexes from mismatched ones.[29–31] Another interesting class of compounds is the monomethine cyanine dyes such as Oxazole yellow (YO) and Thiazole orange (TO). YO has been linked to ODNs[32–33] and TO to peptide nucleic acids (PNA)[34–40] and to ODNs.[41–46] In our previous work, TO was linked to an internucleotidic position on

[a] Dr. R. Lartia, Dr. U. Asseline
Centre de Biophysique Moléculaire, CNRS UPR 4301
affiliated with the University of Orléans and with INSERM
Rue Charles Sadron, 45071 Orleans Cedex 02 (France)
Fax: (+33) 023-863-1517
E-mail: asseline@cnrs-orleans.fr

[b] Dr. R. Lartia
Present address:
Laboratoire de Chimie des Interactions Moléculaires, CNRS, UPR 285
Collège de France. 11 pl. M. Berthelot, 75005 Paris (France)

Supporting information for this article is available on the WWW under http//www.chemeurj.org/ or from the author.

phosphodiester homooligonucleotides.[42,43] These conjugates exhibited a strong increase in fluorescence on hybridization with their target sequences. Among them, the oligo-α-thymidylate–TO conjugates were resistant to nucleases and exhibited unprecedented unaided internalization properties in cultured cells.[43] These interesting results incited us to investigate the possibility of developing ODN probes involving the four nucleic bases and different monomethine cyanine dyes, to obtain conjugates that could be detected at different emission wavelengths. We report here the synthesis and preliminary studies by absorption and fluorescence spectroscopy of new ODN–cyanine conjugates.

Results and Discussion

Experimental design: Cyanine dyes consist of two heterocyclic nuclei containing nitrogen centers linked through an odd number of methine bonds in such a way that resonance occurs through the conjugated system between the tertiary and quaternary nitrogen atoms. Since the synthesis of the first "cyanine" in the mid-1800s, thousands have been used in varied areas.[47–50] These dyes cover the visible and near-infrared spectral regions. The interest in using cyanines as DNA or RNA noncovalent labels[51–56] comes from the work of Lee et al.[57] However, only a few polymethine (Cy3, Cy5, Cy5.3, and Cy5.5) and two monomethine cyanines (TO and YO) have been covalently linked to ODN and PNA probes.[32–46] The interactions of a few other cyanines, including thiocyanine and quinocyanines, with nucleic acids have been investigated and have shown an increase in the fluorescence signal.[58,59] Following this information and our previous results obtained with TO, we chose to synthesize a series of monomethine cyanines and to attach them to various positions on ODNs involving the four nucleic bases.

Cyanines: Monomethine cyanines were chosen because their intercalation between the base pairs of the duplex structures leads to a reduction of rotation around the methine bond, which has been reported to be one of the parameters responsible for the strong increase in fluorescence observed on binding of TO and YO with the DNA duplex.[57,60] The series of the nine selected cyanines (Table 1) includes a thiocyanine (Th), four thiazole orange analogues (2TO, 4TO, 2TO′, and 4TO′), and four quinocyanines (22′Q, 24′Q, 42′Q, and 44′Q). 4TO and 4TO′ correspond to the monomethine cyanines, referred as TO and TO′ in the literature, that have already been linked to peptide nucleic acids[34–40] and homo-ODNs.[41–46] We also synthesized them for the purpose of comparison with the new ODN–cyanine conjugates.

ODN–cyanine conjugates: The fluorescence emission wavelength and intensity of an ODN–label conjugate are not only dependent on the intrinsic properties of the label but also on its different interactions with the environment, including solvents, the ODN itself to which it is linked, and the complex formed between the ODN–label conjugate and its target sequence. Consequently, the fluorescence emission of a label is dependent on the parameters of its linkage to the ODN (position of attachment, base-pair neighbor), as well as the character and length of the linker chosen to connect the two entities. To test the influence of the neighboring base pair on the fluorescence signal on hybridization, the cyanines were attached to the 5′-end of two 14-mer ODNs ending with 5′-CC or 5′-TT sequences (**1** and **2**, Figure 1). These ODNs were complementary to different sequences present on 27-mer target **3**. On the basis of the literature results indicating that the various interactions of cyanines with nucleic acids include intercalation in duplex structures and that most intercalators efficiently stabilize

Table 1. Structures of ODNs and conjugates

ODNs	Sequences
1	$^{5'}$CCGCTTAATACTGA$^{3'}$
2	$^{5'}$TTCTCCCCCGCTTA$^{3'}$
3	$^{5'}$GCGTCAGTATTAAGCGGGGGAGAATTA$^{3'}$
4	$^{5'}p$(S)CCGCTTAATACTGA$^{3'}$
5	$^{5'}p$(S)TTCTCCCCCGCTTA$^{3'}$
$\mathbf{6}_{(R_P,S_P)}$	$^{5'}$CCGCTTA(*p**-R)ATACTGA$^{3'}$ R = $-$NHCH$_2$CH$_2$SSCH$_2$CH$_2$NHAc
$\mathbf{4}_{\mathbf{Th}}$	$^{5'}$**Th-***p*(S)CCGCTTAATACTGA$^{3'}$
$\mathbf{4}_{\mathbf{2TO'}}$	$^{5'}$**2TO'-***p*(S)CCGCTTAATACTGA$^{3'}$
$\mathbf{4}_{\mathbf{4TO'}}$	$^{5'}$**4TO'-***p*(S)CCGCTTAATACTGA$^{3'}$
$\mathbf{4}_{\mathbf{2TO}}$	$^{5'}$**2TO-***p*(S)CCGCTTAATACTGA$^{3'}$
$\mathbf{4}_{\mathbf{22'Q}}$	$^{5'}$**22′Q-***p*(S)CCGCTTAATACTGA$^{3'}$
$\mathbf{4}_{\mathbf{24'Q}}$	$^{5'}$**24′Q-***p*(S)CCGCTTAATACTGA$^{3'}$
$\mathbf{4}_{\mathbf{4TO}}$	$^{5'}$**4TO-***p*(S)CCGCTTAATACTGA$^{3'}$
$\mathbf{4}_{\mathbf{42'Q}}$	$^{5'}$**42′Q-***p*(S)CCGCTTAATACTGA$^{3'}$
$\mathbf{4}_{\mathbf{44'Q}}$	$^{5'}$**44′Q-***p*(S)CCGCTTAATACTGA$^{3'}$
$\mathbf{5}_{\mathbf{Th}}$	$^{5'}$**Th-***p*(S)TTCTCCCCCGCTTA$^{3'}$
$\mathbf{5}_{\mathbf{2TO'}}$	$^{5'}$**4TO'-***p*(S)TTCTCCCCCGCTTA$^{3'}$
$\mathbf{5}_{\mathbf{2TO}}$	$^{5'}$**2TO-***p*(S)TTCTCCCCCGCTTA$^{3'}$
$\mathbf{5}_{\mathbf{22'Q}}$	$^{5'}$**22′Q-***p*(S)TTCTCCCCCGCTTA$^{3'}$
$\mathbf{5}_{\mathbf{24'Q}}$	$^{5'}$**24′Q-***p*(S)TTCTCCCCCGCTTA$^{3'}$
$\mathbf{5}_{\mathbf{4TO}}$	$^{5'}$**4TO-***p*(S)TTCTCCCCCGCTTA$^{3'}$
$\mathbf{6}_{\mathbf{Th}R_P}$	$^{5'}$CCGCTTA(*p**-NHCH$_2$CH$_2$S-**Th**)ATACTGA$^{3'}$
$\mathbf{6}_{\mathbf{Th}S_P}$	$^{5'}$CCGCTTA(*p**-NHCH$_2$CH$_2$S-**Th**)ATACTGA$^{3'}$
$\mathbf{6}_{\mathbf{4TO'}R_P}$	$^{5'}$CCGCTTA(*p**-NHCH$_2$CH$_2$S-**4TO'**)ATACTGA$^{3'}$
$\mathbf{6}_{\mathbf{4TO'}S_P}$	$^{5'}$CCGCTTA(*p**-NHCH$_2$CH$_2$S-**4TO'**)ATACTGA$^{3'}$
$\mathbf{6}_{\mathbf{4TO}R_P}$	$^{5'}$CCGCTTA(*p**-NHCH$_2$CH$_2$S-**4TO**)ATACTGA$^{3'}$
$\mathbf{6}_{\mathbf{4TO}S_P}$	$^{5'}$CCGCTTA(*p**-NHCH$_2$CH$_2$S-**4TO**)ATACTGA$^{3'}$
$\mathbf{6}_{\mathbf{44'Q}R_P}$	$^{5'}$CCGCTTA(*p**-NHCH$_2$CH$_2$S-**44′Q**)ATACTGA$^{3'}$
$\mathbf{6}_{\mathbf{44'Q}S_P}$	$^{5'}$CCGCTTA(*p**-NHCH$_2$CH$_2$S-**44′Q**)ATACTGA$^{3'}$

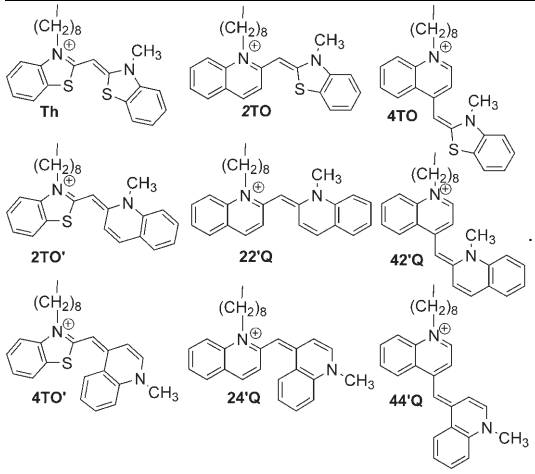

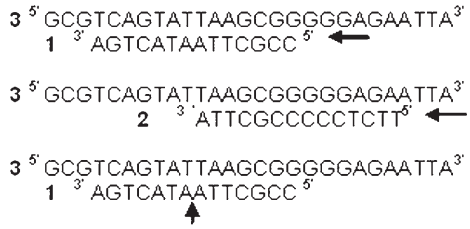

Figure 1. Structure of the duplexes (**1**+**3** or **2**+**3**). The arrows indicate the linkage positions of the cyanines

duplex structures when linked to ODNs by linkers whose size is at least 5–6 methylene groups,[61,62] we used an octamethylene linker to attach them to the 5′-ends of the ODNs. Nine cyanines were attached to ODN **1** and six (Th, 4TO, 2TO, 2TO′, 22′Q, and 24′Q) to ODN **2**. Since our previous work showed that TO cannot withstand the basic conditions required for deprotection of an ODN involving the four nucleic bases, we chose to link the cyanines to the ODNs by a reaction between a thiophosphate incorporated at the 5′-end of ODNs **1** and **2**[63,64] and a iodoalkyl group present on the cyanine-linker derivatives.

Four cyanines (Th, 4TO, 4TO′, and 44′Q) corresponding to different combinations of the benzothiazole and lepidine moieties were also attached to the central phosphate of the 14-mer ODN **1** between two 2′-deoxyadenosines. This linkage induced the formation of two isomers leading to two different positions on the cyanines on hybridization of the conjugates with the complementary sequence. For one isomer the ligand protrudes into the minor groove of the duplex, while for the other the ligand is directed towards the major groove. Because our previous work showed that good stabilization of a duplex by an intercalator linked to an internucleotidic phosphate requires a longer linker (at least eleven atoms) than when attached to the termini of ODNs, we used a twelve-atom linker.[65,66]

Synthesis

*Synthesis of cyanine-linker derivatives **9–17***: Syntheses of cyanine-linker derivatives **9**–**17**, adapted from reported procedures,[51,67–69] were achieved by reaction of two heterocyclic quaternary salts (Scheme 1, Table 2). One bore a methyl group (**7a–c**) which could be deprotonated to give a methylene derivative acting as a nucleophilic reagent. The other had a good leaving group, either a thioalkyl group (**8a**) or an halogen atom (**8b**,**c**). The cyanine-linker derivatives can be classified into three series. In compounds **9**–**11**, the iodooctyl linker is attached to the nitrogen atom of the benzothiazole ring, in compounds **12**–**14**, to the nitrogen atom of quinaldine, and in compounds **15**–**17**, to the nitrogen atom of lepidine.

N-(8-Iodooctyl)-2-methylbenzothiazolium iodide (**7a**) was obtained by alkylation of the nitrogen atom of 2-methylbenzothiazole with 1,8-diiodooctane. Compound **7a** was then treated with **8a**[51] to give thiocyanine **9**, with **8b** to give cyanine **10**, and with **8c** to afford cyanine **11**. Other cyanine-linker derivatives were obtained by following the same synthetic pathway as indicated in Table 1. Pure cyanines were obtained with yields ranging from 20 to 50% (see Experimental Section) and characterized by ^{1}H NMR, ^{13}C NMR, and mass spectrometric analyses. They can easily be distinguished by their characteristic =CH− and N^+Me chemical shifts in the 6.14–7.09 ppm and 4.02–4.42 ppm regions, respectively.

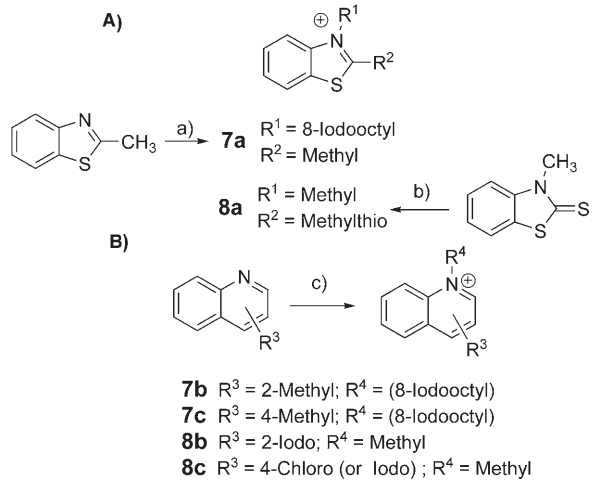

Scheme 1. Synthesis of heterocyclic quaternary salts bearing an acidic methyl group **7a–c** and those bearing a leaving group **8a–c**. A): Benzothiazole-containing compounds. B): Quinoline-containing compounds. Reagents and conditions: a) $I(CH_2)_8I$ (5 equiv), 150°C; b) CH_3I, MeOH, reflux; c) $I(CH_2)_8I$ (5 equiv), dioxane, reflux (for **7b–c**); MeI, MeOH, 50°C (for **8b–c**).

Table 2. Preparation of the cyanine-linker derivatives RI (**9–17**).[a]

Reagents	8a	8b	8c
7a	**9** (**Th**)	**10** (**2TO′**)	**11** (**4TO′**)
7b	**12** (**2TO**)	**13** (**22′Q**)	**14** (**24′Q**)
7c	**15** (**4TO**)	**16** (**42′Q**)	**17** (**44′Q**)

[a] 8-Iodooctyl-containing cyanines **9**–**17** were obtained by reaction between **7a–c** and **8a–c** in MeOH/CH_2Cl_2 or MeOH/$ClCH_2CH_2Cl$ (50/50) mixture with TEA as basic reagent.

Synthesis of modified ODN conjugates bearing the cyanine at the 5′-end: The synthesis of the conjugates involving the cyanines linked to the 5′-ends of the ODNs (Scheme 2 A) relies on the incorporation of a thiophosphate group at the 5′-terminal position of the ODN bound to the support by our previously reported method.[64] After the deprotection step, the crude 5′-thiophosphorylated ODNs **4** and **5** were allowed to react with the iodoalkyl groups of the cyanines in methanol in the presence of crown ether to solubilize the ODNs. ODN **4** was treated with the nine cyanines **9** to **17** to give the ODN–cyanine conjugates $\mathbf{4}_{\mathbf{Th\text{-}44'Q}}$. ODN **5** was treated with six cyanines **9**, **10**, and **12**–**15** to give the ODN–cyanine conjugates $\mathbf{5}_{\mathbf{Th}}$, $\mathbf{5}_{\mathbf{2TO}}$, $\mathbf{5}_{\mathbf{22'Q}}$, $\mathbf{5}_{\mathbf{4TO'}}$, $\mathbf{5}_{\mathbf{4TO}}$, and $\mathbf{5}_{\mathbf{24'Q}}$ (see Table 1 for structures). The conjugates were purified by reversed-phase chromatography (see Figure 2 and Table 3),

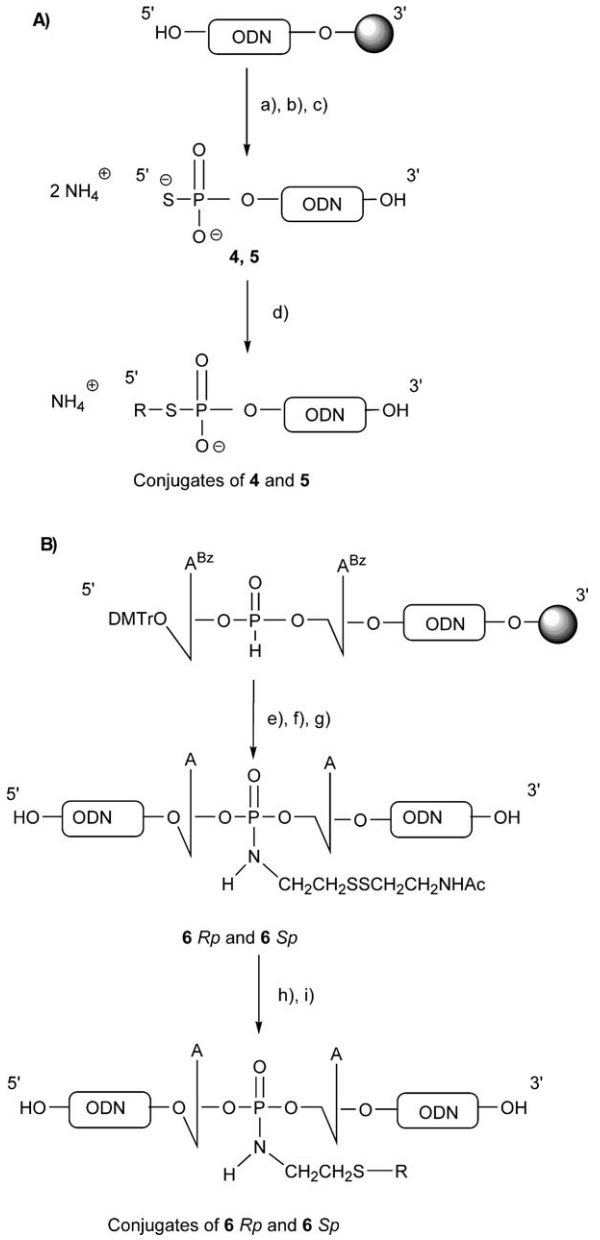

Scheme 2. General synthetic procedure for the preparation of conjugates. A): 5′-labeling; B): internucleotidic labeling. Reagents: a) See ref. [64]; b) S_8, CS_2/C_5H_5N; c) NH_4OH, overnight, 55 °C; d) RI (among **9**–**17**), [18]crown-6 in MeOH 6 h, RT; e) cystamine, CCl_4, C_5H_5N; f) Ac_2O, 4-dimethylaminopyridine (DMAP), C_5H_5N, CH_3CN; g) chain elongation; NH_4OH, 50 °C, overnight; h) purification and isomer separation; i) Ar, TCEP, RI (**9**, **11**, **15**, or **17**), DMF, $NaHCO_3$ 0.5 %, pH 9.

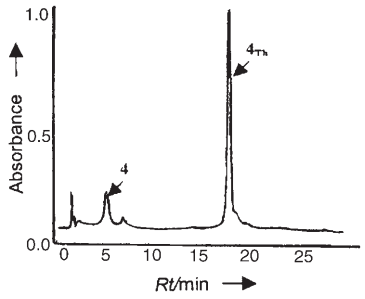

Figure 2. Reversed-phase HPLC analysis of the coupling reaction between ODN **4** and cyanine-linker derivative **9** performed on a Lichrospher R_P 18 (5 μm) column (125 mm × 4 mm) from Merck with a linear gradient of CH_3CN (12 to 35 % over 30 min) in 0.1 M aqueous triethylammonium acetate (TEAA), pH 7, with a flow rate of 1 mL min^{-1}. Detection at $\lambda = 260$ nm.

Table 3. Characterizations of conjugates.

	Retention time[a]	Mass analysis	
		calcd	found
$\mathbf{6}_{R_P}$	10 min 35 s	4399.02	4399.02
$\mathbf{6}_{S_P}$	11 min 14 s	4399.02	4398.64
$\mathbf{4}_{\mathbf{Th}}$	11 min 28 s	4725.46	4725.39
$\mathbf{4}_{\mathbf{2TO'}}$	11 min 58 s	4719.46	4719.02
$\mathbf{4}_{\mathbf{4TO'}}$	12 min 07 s	4719.46	4718.05
$\mathbf{4}_{\mathbf{2TO}}$	11 min 22 s	4719.46	4719.11
$\mathbf{4}_{\mathbf{22'Q}}$	13 min 17 s	4713.42	4712.17
$\mathbf{4}_{\mathbf{24'Q}}$	13 min 26 s	4713.42	4713.17
$\mathbf{4}_{\mathbf{4TO}}$	11 min 28 s	4719.46	4718.84
$\mathbf{4}_{\mathbf{42'Q}}$	12 min 53 s	4713.42	4712.23
$\mathbf{4}_{\mathbf{44'Q}}$	12 min 48 s	4713.42	4712.32
$\mathbf{5}_{\mathbf{Th}}$	15 min 04 s	4628.38	4628.38
$\mathbf{5}_{\mathbf{2TO'}}$	15 min 36 s	4622.38	4622.03
$\mathbf{5}_{\mathbf{2TO}}$	15 min 28 s	4622.38	4622.84
$\mathbf{5}_{\mathbf{22'Q}}$	17 min 12 s	4616.34	4615.38
$\mathbf{5}_{\mathbf{24'Q}}$	17 min 21 s	4616.34	4615.74
$\mathbf{5}_{\mathbf{4TO}}$	16 min 42 s	4622.38	4622.02
$\mathbf{6}_{\mathbf{Th}R_P}$	18 min 09 s	4689.02	4703.93
$\mathbf{6}_{\mathbf{Th}S_P}$	20 min 03 s	4689.02	4687.92
$\mathbf{6}_{\mathbf{4TO'}R_P}$	17 min 19 s	4683.55	4698.48
$\mathbf{6}_{\mathbf{4TO'}S_P}$	21 min 18 s	4683.55	4696.32
$\mathbf{6}_{\mathbf{4TO}R_P}$	16 min 40 s	4683.55	4699.26
$\mathbf{6}_{\mathbf{4TO}S_P}$	19 min 20 s	4683.55	4698.56
$\mathbf{6}_{\mathbf{44'Q}R_P}$	18 min 22 s	4677.53	4676.95
$\mathbf{6}_{\mathbf{44'Q}S_P}$	21 min 43 s	4677.53	4676.67

[a] Retention times obtained by reversed-phase HPLC analyses for ODNs $\mathbf{6}_{R_P}$, $\mathbf{6}_{S_P}$, and ODN–cyanine conjugates performed under the same column and buffer conditions as in Figure 2 by using a linear gradient of CH_3CN (16 to 40 % over 40 min for conjugates **4** and **5**, and 8 to 28 % over 25 min for ODNs $\mathbf{6}_{R_P}$, $\mathbf{6}_{S_P}$ and their conjugates). Detection at $\lambda =$ 260 nm.

and characterized by electrospray mass spectrometry (Table 3) and UV/Vis spectroscopy (Figure 3). The visible absorption bands of the different conjugates span from 429 to 595 nm.

Synthesis of ODN conjugates with cyanines linked to an internucleotidic phosphate: Modified ODNs $\mathbf{6}_{\mathbf{Th}}$, $\mathbf{6}_{\mathbf{TO}}$, $\mathbf{6}_{\mathbf{TO'}}$, and $\mathbf{6}_{\mathbf{44'Q}}$ (Scheme 2B) were synthesized as previously reported for ODN–TO conjugates.[42] This method relies on the incorporation, during ODN chain elongation, of a cystamine group[70] at the position chosen for the linkage of the cyanines to give ODN–linker derivative isomers $\mathbf{6}_{R_P}$ and $\mathbf{6}_{S_P}$, which were separated by reversed-phase chromatography. Each series of pure conjugates was then obtained by a reaction between *N*-(8-iodooctyl)-cyanines **9**, **11**, **15**, and **17** and the thiol function released on cleavage of the disulfide bridge of the cystamine by treatment with a reducing agent.[71] The conjugate isomers $\mathbf{6}_{\mathbf{Th}}$, $\mathbf{6}_{\mathbf{4TO}}$, $\mathbf{6}_{\mathbf{4TO'}}$, and $\mathbf{6}_{\mathbf{44'Q}}$ were

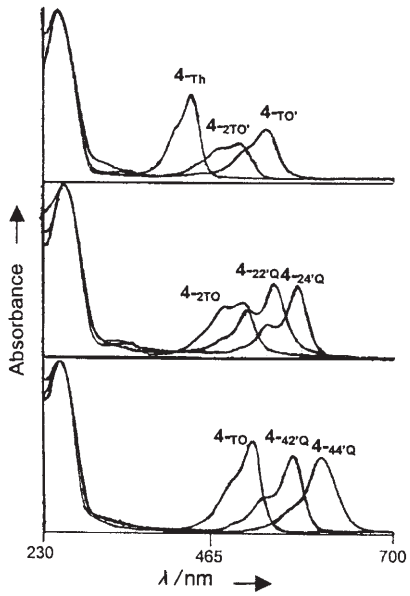

Figure 3. UV/Vis absorption spectra of the nine conjugates of ODN **4** recorded between $\lambda = 230$ and 600 nm in a 10 mM sodium cacodylate, pH 7, buffer containing 100 mM NaCl.

purified by reversed-phase chromatography and analyzed by electrospray mass spectrometry (Table 3).

Isomer identification: Isomers were identified on the basis of our previous results.[42] When subjected to nuclease degradation by endonuclease P1 (or S1) and alkaline phosphatase, each isomer of ODN **6** gave the four mononucleosides dC, dG, dT, dA and the dinucleotide-linker derivative isomer d-$^{5'}$Ap*-[N(H)$(CH_2)_2$SS-$(CH_2)_2$N(H)C(O)OCH_3]-dA$^{3'}$. The relative elution order was the same for both isomers of ODN **6** and the corresponding dinucleotide isomers. In our previous work, we demonstrated that the R_P isomer of the dinucleotide linker derivative d-$^{5'}$Ap*[N(H)$(CH_2)_2$-SS-$(CH_2)_2$N(H)C(O)OCH_3]-dA$^{3'}$ was eluted faster than the S_P isomer. We can conclude that oligonucleotide-linker conjugate **6** eluted first has the R_P configuration. After coupling of the various cyanines with each pure ODN-linker isomer $\mathbf{6}_{R_P}$ and $\mathbf{6}_{S_P}$, reversed-phase analysis confirmed that all the ODN–cyanine conjugates coming from the R_P isomer of the ODN–linker derivative **6** eluted earlier than the corresponding ODN–cyanine conjugates from the S_P isomer. Therefore, for each pair of ODN–cyanine conjugates, the compound eluted first has the R_P configuration. This result is in agreement with the literature that, in ODNs involving an internucleotidic group appended via a phosphoramidate linkage, the faster eluting isomer in reversed-phase chromatography shows the R_P configuration.[72,73]

UV/Vis absorption spectroscopy

Free probes: The spectra of the nine conjugates derived from ODN **4** are shown in Figure 3. In all cases, the spectra contain an absorption band in the UV range corresponding to the absorbance of the ODN and the cyanine, while the absorption band in the visible range corresponds to only that of the cyanine. The λ_{max} values of the UV and visible absorption bands are given in Table 4. The intensity ratios of the UV/Vis bands also depend on the cyanine considered (Figure 3). A comparison of the three series of conjugates derived from ODNs **4**, **5**, and **6** showed that for each cyanine, the visible λ_{max} was slightly different, depending on the ODN sequence. The λ_{max} of conjugates **5** were blue-shifted compared to λ_{max} of the conjugates of **4** involving the same cyanine. This reflects the stronger interaction of the dye with its ODN counterpart due to a higher purine/pyrimidine

Table 4. Spectroscopic data for conjugates.[a]

ODN	λ_{UVmax} [nm]	ε[b] [$M^{-1}cm^{-1}$]	λ_{VISmax} [nm]	ε[b] [$M^{-1}cm^{-1}$]	T_m [°C]	ΔT_m (±0.5 °C)
1	261				43.5	
2	269				51.5	
$\mathbf{4}_{Th}$	260	149100	430	79000	51.2	+7.7
$\mathbf{4}_{2TO'}$	259	147000	492	34500	50.5	+7.0
$\mathbf{4}_{4TO'}$	259	170000	514	51700	51.0	+7.5
$\mathbf{4}_{2TO}$	259	173800	495	57100	54.0	+10.5
$\mathbf{4}_{22'Q}$	259	136100	528	56200	53.0	+9.5
$\mathbf{4}_{24'Q}$	258	137100	563	60000	52.0	+8.5
$\mathbf{4}_{4TO}$	262	143100	515	73500	48.0	+4.5
$\mathbf{4}_{42'Q}$	259	135900	563	67000	49.0	+5.5
$\mathbf{4}_{44'Q}$	259	136800	595	46000	47.5	+4.0
$\mathbf{5}_{Th}$	268	131200	429		57.0	+5.5
$\mathbf{5}_{2TO'}$	268	129100	488		56.0	+4.5
$\mathbf{5}_{2TO}$	267	155900	490		58.0	+6.5
$\mathbf{5}_{22'Q}$	266	118200	525		56.5	+5.0
$\mathbf{5}_{24'Q}$	266	119200	562		57.0	+5.5
$\mathbf{5}_{4TO}$	267	125200	511		55.5	+4.0
$\mathbf{6}_{Th R_P}$	261	149100	430		44.5	+1.0
$\mathbf{6}_{Th S_P}$	261	149100	430		46.5	+3.0
$\mathbf{6}_{4TO' R_P}$	259	170000	512		44.0	+0.5
$\mathbf{6}_{4TO' S_P}$	258	170000	512		50.0	+6.5
$\mathbf{6}_{4TO R_P}$	261	143100	512		47.5	+4.0
$\mathbf{6}_{4TO S_P}$	261	143100	514		45.0	+1.5
$\mathbf{6}_{44'Q R_P}$	255	136800	595		47.5	+4.0
$\mathbf{6}_{44'Q S_P}$	258	136800	595		43.5	0

[a] The experiments were performed with 1 μM concentration in ODN (each strand) in a 10 mM sodium cacodylate buffer pH 7 containing 100 mM NaCl. [b] ε values were determined experimentally for conjugates $\mathbf{4}_{Th}$–$\mathbf{4}_{44'Q}$. The same values were used for the corresponding conjugates **6** involving the same sequence. For conjugates **5** the ε values at $\lambda = 260$ nm were the approximate sum of the ε values of the ODN and of cyanines deducted from those of conjugates **4.**

ratio in conjugates **4**, as previously reported in the case of PNA–4TO′ conjugates.[37] ODNs **4** and **6** not only have the same base composition and sequence but also a very similar λ_{max}. The covalent attachment of the cyanines in conjugates **4** is adjacent to two cytosine residues whereas it is adjacent to two adenine residues for conjugates **6**. This result suggests that in the free conjugates, the cyanines not only interact with bases adjacent to their attachment position on the ODN sequence but also with different bases throughout the sequence due to the flexibility of the ODN chain.

Determination of the molar extinction coefficients: The molar extinction coefficients ε for conjugates $\mathbf{4_{Th}}$–$\mathbf{4_{44'Q}}$ were determined by titration of their solutions with complementary DNA target **3** (Table 4 and Experimental Section). The ε_{260} value for ODN **3** was determined by using the nearest-neighbor model.[74] A comparison of the ε values at λ_{max} for each pair of isomers $\mathbf{4_{2TO}}/\mathbf{4_{2TO'}}$, $\mathbf{4_{4TO}}/\mathbf{4_{4TO'}}$, and $\mathbf{4_{24'Q}}/\mathbf{4_{42'Q}}$ shows the influence of the structure on the spectroscopic properties. For a given dye, depending on the heterocyclic nucleus bearing the linker arm, different ε values were observed. The highest values were obtained when the linker was attached to the 4-position of the quinoline nucleus. This also reflects the different interactions of the cyanines with the ODN sequence to which they are attached as a function of the cyanine structure and the anchoring position of the linker on the cyanine. The same values were used for the corresponding conjugates **6** involving the same sequence and the same cyanines. For conjugates **5**, the ε values at 260 nm were approximated as the sum of the ε values of ODN **2**, determined by using the nearest-neighbor model,[74] and of the cyanines deducted from those of conjugates **4.**

Hybridized probes: Since a DNA duplex is more rigid than a single-stranded sequence, it is likely that on hybridization of the conjugate series **4** and **5** with target sequence **3**, the cyanines will be able to interact with only the end of the duplex and a few bases on the overhanging single-stranded target adjacent to the duplex on the side of the cyanine attachment. Due to the choice of target sequences (Figure 1), the cyanines are located in an environment containing only G and C bases for conjugates **4**, and only A and T bases for conjugates **5**. On hybridization of conjugates **6** with target sequence **3**, the cyanines can only interact with a duplex in the vicinity of their attachment position in an environment containing only A and T bases. Mixing equimolar amounts of the conjugates and target **3** at 3 °C induces modifications of their absorption spectra that are reversed on increasing the temperature to 65 °C. In any case, except for the S_P isomer of conjugate $\mathbf{6_{44'Q}}$, the presence of the cyanines stabilizes the duplexes as compared to the unmodified references (Table 4). However, the difference in stabilization observed depends on many parameters such as the position of their attachment to the ODN, the neighboring base pairs, and the cyanines. More specifically, the following observations have been made.

5′-conjugated ODNs: For conjugates derived from ODN **4**, the main changes observed were hypochromism (6–19 %, except in the case of $\mathbf{4_{44'Q}}$, for which 50 % hypochromism was observed) with a very weak blue shift (data not shown). This strong hypochromism could be due to hydrogen-bond formation between the uncharged nitrogen atom of the cyanine and a hydrogen atom of the duplex. Thermal denaturation experiments indicated that the greatest stabilization was obtained with the cyanines attached via the quinaldine ring ($\Delta T_m = +10.5$, $+9.5$, and $+8.5$ °C, respectively; See Table 4 and Figure 4). Stabilization was moderate when the cyanines were attached through the benzothiazole ring ($\Delta T_m = +7.7$, $+7$, and $+7.5$ °C, respectively), and lowest when the cyanines were linked through the lepidine ring ($\Delta T_m = +4.5$, $+5.5$, and $+4$ °C, respectively).

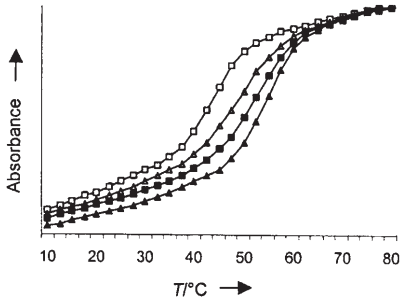

Figure 4. UV/melting curves (normalized) for duplexes **4**+**3** (□), $\mathbf{4_{44'Q}}$+**3** (△), $\mathbf{4_{2TO'}}$+**3** (■), and $\mathbf{4_{2TO}}$+**3** (▲), recorded at $\lambda = 260$ nm. See Table 4 for conditions.

In the case of conjugates **5**, the main changes in the absorption spectra also concerned the intensities (a 4–8 % decrease, data not shown). Considering the same cyanines, the stabilities observed with conjugates **5** were lower than those obtained with conjugates **4**, and the greatest stabilization was obtained with conjugates $\mathbf{5_{2TO}}$, $\mathbf{5_{22'Q}}$, and $\mathbf{5_{24'Q}}$, in which the cyanines are attached to the ODN via the quinaldine ring (Table 4; $\Delta T_m = +6.5$, $+5$, and $+5.5$ °C, respectively). These stabilization values are only slightly superior to those observed with the other conjugates **5**.

For each of the three series of cyanines, the values of the dihedral angle along the chromophore chain were different (see Figure 5). Of the cyanines, those in which the second heterocyclic nucleus is attached at the 2-position of the

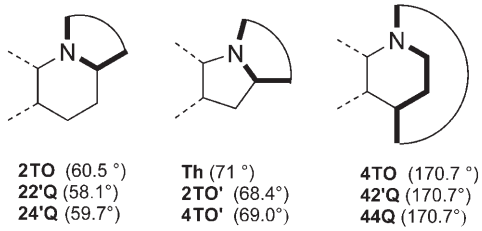

Figure 5. Schematic representation of the different dihedral angles (in bold lines) for the three series of cyanines, and values obtained by MM2 calculations.

quinoline bearing the linker (**2TO**, **22′Q**, and **24′Q**) provide the strongest stability and have smaller dihedral angles (60.5, 58.1, and 59.7°) probably due to a better stacking with the neighboring base pairs. However, the strongest stabilization was observed with conjugates **4** in which the cyanines were forced to interact with a neighboring CG base pair on duplex formation. Since AT base pairs at the end of a duplex are less tightly bound than terminal GC pairs, more efficient stacking is likely to occur with the latter.

Conjugates **6** *with cyanines attached to an internucleotidic phosphate*: On binding of conjugates **6** with target sequence **3**, the main spectral change observed was hypochromism ranging from 7 to 20% and reaching 44% in the case of the S_P isomer of conjugate $\mathbf{6}_{\mathbf{44'Q}}$. Comparison of the T_m values indicated that when the cyanines were attached via the benzothiazole ring (**Th** and **4TO′**) the strongest stabilization was obtained with the S_P isomers ($\Delta T_m = +3$ and $+6.5$ °C, respectively) in which the label is directed towards the major groove, while the greatest stabilization was observed with the R_P isomers ($\Delta T_m = +4$ °C and $+4$ °C, respectively) in which the label is directed towards the minor groove, when the cyanines are attached via the lepidine ring (**4TO** and **44′Q**) (Figure 6).

These results agree with an NMR study indicating that the TO dimer TOTO intercalated in duplex DNA through the minor groove with the lepidine ring located between two purines.[75] They are also consistent with our previous result[42] indicating that in the S_P isomer of the oligo-2′-deoxyadenylates, the linker points towards the major groove and probably folds back in the direction of the minor groove because it does not prevent binding of a third strand in the major groove of the duplex.

Fluorescence studies on ODN-cyanine conjugates: Steady-state fluorescence experiments were performed under the same conditions (concentration, buffer) as for the T_m measurements (see Experimental Section and Table 5).

Free conjugates ***4*** *and* ***5***: As can be seen from Table 5, λ_{em} for conjugates **4** and **5** ranges from 453 nm for $\mathbf{4}_{\mathbf{Th}}$ to 610 nm for $\mathbf{4}_{\mathbf{44'Q}}$ with little difference between the two series. Comparison of the fluorescence intensities observed for conjugates **4** and **5** (taking into account the difference in absorbance at λ_{exc} for each conjugate; data not shown) indicated that they depend on cyanine composition. The thiocyanines were the most fluorescent followed by the conjugates linked to **4TO**, and the conjugates involving quinocyanines were the least fluorescent. A comparison of the results obtained with the two series of conjugates **4** and **5** indicated that **Th**, **2TO′**, and **2TO** were more fluorescent when linked to the purine-rich sequence **4**, while cyanine 4TO was more fluorescent when linked to the pyrimidine-rich sequence. Conjugates **4** contain 8 pyrimidines and 6 purines (including two guanines), and conjugates **5** contain 12 pyrimidines and 2 purines (including one guanine). However, the two terminal bases at the 5′-end of conjugates **4** and **5** are pyrimidines. Since both C and T have similar reduction potentials,[76,77] the differences observed could be due to interaction of the cyanines with the other nucleic bases of the sequences.

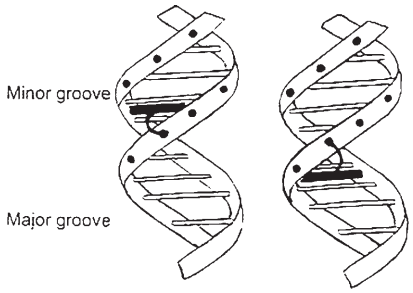

Figure 6. Schematic representation of the duplexes formed between ODN **3** and conjugates $\mathbf{6}_{\mathbf{4TO}R_P}$ (left) and $\mathbf{6}_{\mathbf{4TO'}S_P}$ (right). The black rectangles stand for the cyanines.

Table 5. Fluorescence data for conjugates.[a]

ODN	Free conjugate				Duplex		I_F(Duplex)/
	λ_{ex} [nm]	λ_{em} [nm]	Stokes shift	I_F[b]	λ_{em} [nm]	I_F[b,c]	I_F(conjugate)
$\mathbf{4}_{\mathbf{Th}}$	431	453	22	59.1	455	33	0.56
$\mathbf{4}_{\mathbf{2TO'}}$	493	523	30	6.6	[c]	2.2	0.33
$\mathbf{4}_{\mathbf{4TO'}}$	517	532	15	8.8	530	8.4	0.95
$\mathbf{4}_{\mathbf{2TO}}$	497	521	24	13.7	523	6.28	0.45
$\mathbf{4}_{\mathbf{22'Q}}$	525	[d]	nd	0.5	[c]	0.43	0.86
$\mathbf{4}_{\mathbf{24'Q}}$	562	569	7	1.6	570	1.33	0.83
$\mathbf{4}_{\mathbf{4TO}}$	516	529	13	23.2	529	10	0.43
$\mathbf{4}_{\mathbf{42'Q}}$	560	570	10	2.1	571	0.96	0.45
$\mathbf{4}_{\mathbf{44'Q}}$	595	610	15	1.2	608	1.17	0.97
$\mathbf{5}_{\mathbf{Th}}$	430	462	32	41.9	466	28.2	0.67
$\mathbf{5}_{\mathbf{2TO'}}$	492	[d]	nd	3.8	_[d]	2.7	0.71
$\mathbf{5}_{\mathbf{2TO}}$	494	524	30	7.9	528	4.4	0.55
$\mathbf{5}_{\mathbf{22'Q}}$	nd	nd	nd	nd	nd	nd	nd
$\mathbf{5}_{\mathbf{24'Q}}$	562	573	11	5.4	573	4.4	0.82
$\mathbf{5}_{\mathbf{4TO}}$	513	528	15	37.6	528	27.0	0.74
$\mathbf{6}_{\mathbf{Th}R_P}$	430	458	28	57.6	461	80.4	1.39
$\mathbf{6}_{\mathbf{Th}S_P}$	431	456	25	71.4	447	93.8	1.31
$\mathbf{6}_{\mathbf{4TO'}R_P}$	514	532	18	10.6	527	14.1	1.33
$\mathbf{6}_{\mathbf{4TO'}S_P}$	516	533	17	17.3	526	46.9	2.71
$\mathbf{6}_{\mathbf{4TO}R_P}$	513	531	18	32.7	521	79.2	2.42
$\mathbf{6}_{\mathbf{4TO}S_P}$	516	531	15	51.2	523	40.2	0.79
$\mathbf{6}_{\mathbf{44'Q}R_P}$	594	611	17	5.0	601	2.5	0.50
$\mathbf{6}_{\mathbf{44'Q}S_P}$	595	614	19	13.8	605	3.0	0.22

[a] The experiments were performed with 1μM concentration in ODN (each strand) in a 10 mM sodium cacodylate buffer pH 7 containing 100 mM NaCl. [b] Arbitrary units ($\times 10^6$). Studies were performed at 5°C. [c] Values were corrected for the changes in absorbance observed on duplex formation. [d] Because of a too-broad band, the determination of λ_{em} was difficult. nd = not determined.

*Free conjugates **6** with cyanines attached to an internucleotidic phosphate*: The λ_{em} are nearly identical for each pair of conjugates **6**, and nearly identical to those of conjugates **4** involving the same cyanine (Table 5). However, internally labeled ODN isomers **6** were more fluorescent than the conjugates **4** sharing the same base sequence, and the S_P isomers were more fluorescent than the R_P ones. This increase in fluorescence intensity could be due to several parameters. First, the cyanine was linked between two A, and our previous results on homo-ODN–thiazole orange conjugates showed that linkage of the label at the internucleotidic position of oligo-2′-deoxyriboadenylates gave more fluorescent conjugates than did the linkage at the internucleotidic position of oligothymidylates.[43,44] Secondly, the size of the linker was larger than that used to connect the cyanines at the 5′-end of the ODNs. Finally, it can be assumed that rotation around the methine bond was more restricted when the cyanine dyes were linked to the central phosphate of a 14-mer ODN, rather than to its terminal phosphate. The largest Stoke shift values were obtained for the cyanines involving one or two benzothiazole rings.

*Hybridized conjugate ODNs **4** and **5***: On hybridization of conjugates **4** and **5** with the target sequence there were either no changes or a very slight shift of λ_{em} together with a decrease in the fluorescence signal (Table 5). The decrease was greater for conjugates **4** than for conjugates **5.** We assume that such differences could be explained by different quenching rates of the cyanine dyes by the neighboring nucleobases (dGdG in **4** and dAdT in **5**).[77] Since the increase in thermal stability of the duplexes formed with the conjugates was substantial compared to that of the parent duplex, it cannot be explained only by the charge neutralization due to the positive charge present on the cyanines. It is likely that, if not perfectly intercalated, the cyanines were stacked at the end of the duplex at the duplex/single strand junction. Efficient stacking of the cyanines with the neighboring base pairs is also consistent with the strong quenching of fluorescence observed for the conjugates **4** and **5**.

*Hybridized conjugates **6** with cyanines attached to an internucleotidic phosphate group*: For the series of ODN isomers **6**, various intensity changes of the fluorescence signal were obtained, ranging from a moderate increase to an pronounced decrease, depending on the isomer and the cyanine used. It is particularly interesting to compare the fluorescence intensities of the duplexes involving ODNs $\mathbf{6_{4TO}}$ and $\mathbf{6_{4TO'}}$. For the $\mathbf{6_{4TO}}$ derivatives, hybridization of the R_P isomer led to a moderate increase (2.4-fold), while that of the S_P isomer induced a moderate decrease (20%). Even though the change in intensity was weaker than that of the oligo-2′-desoxyriboadenylate–**TO** conjugates,[44] an increase was observed for the R_P isomer. In these conjugates, the cyanine was connected to the ODN through its quinoline ring. In contrast, for the $\mathbf{6_{4TO'}}$ derivatives, hybridization of the R_P isomer led to a weak increase (33%), while that of the S_P isomer induced a greater increase (twofold). This corresponds to linkage of the cyanine to the ODN chain through the benzothiazole ring. Our results are consistent with NMR studies showing that **TO** intercalates through the minor groove between two purines and with literature results, published during the course of this work, showing that **4TO′** is able to thread an attached peptide into the major groove, whereas the other groove can be targeted by **4TO**-appended peptides.[78] Other recent reports showed that when **4TO** and **4TO′** are used as base surrogates in PNA probes, the fluorescence changes observed on hybridization depend on the position of attachment of the linker to the cyanines.[40] For conjugates $\mathbf{6_{Th}}$, the cyanine was attached to the ODN via the benzothiazole ring as for the conjugates $\mathbf{6_{4TO'}}$. A slightly more stable duplex was obtained with the S_P isomer than with the R_P isomer. A moderate increase in fluorescence intensity was observed for both isomers. For conjugates $\mathbf{6_{Th}}$, contrary to what was observed with the other pairs of isomer conjugates, a large difference in λ_{em} was observed between both isomers on duplex formation as compared to λ_{em} of the corresponding free probes (Table 5). For conjugates $\mathbf{6_{44'Q}}$, the cyanine is linked to the ODN via a quinoline ring as for conjugates $\mathbf{6_{4TO}}$, and a decrease in the fluorescence intensity was observed for both isomers of $\mathbf{6_{44'Q}}$.

Conclusion

This work reports the synthesis and properties of new ODN–cyanine conjugates. Nine monomethine cyanines displaying either different ring compositions or relative positions on the heterocyclic nuclei and exhibiting different shapes and emission wavelengths have been synthesized (**9**–**17**). These cyanines were covalently linked, via an octamethylene linker, to the 5′-end of 14-mer ODN **4** involving the four nucleic bases and ending at the 5′-terminus with two cytosines. Until now only cyanines **11** and **15** have been covalently linked to PNA and cyanine **15** to ODNs. They were used for the purposes of comparison. Six out of nine cyanines (**9**, **10** and **12**–**15**) were also linked to the 5′-end of another 14-mer ODN **5** ending at the 5′-terminus with two thymines. To study the influence of the attachment position of the cyanines to the ODN chain, four of them (**9**, **11**, **15**, **17**) were attached to the central phosphate of the 14-mer ODN **6** involving the same sequence as ODN **4.** The linker was attached to the central phosphate located between two 2′-deoxyadenosines. This linkage induced the formation of two isomers and thus two different positions of the cyanines on hybridization of the conjugates with the complementary sequence. For one isomer, the ligand protruded into the minor groove of the duplex, while it was directed towards the major groove for the second isomer. Two series of ODN conjugate isomers **6** were obtained as pure isomers. For all the conjugates, except for the S_P isomer of $\mathbf{6_{44'Q}}$, duplex stabilization due to the presence of the cyanines was observed. This stabilization greatly depended on the shape of the cyanines and on the parameters of their linkage to the ODNs. Steady-state fluorescence studies indicated that these cya-

nines exhibited emission signals ranging from 450 to 610 nm. In all cases, a change in the intensity of the fluorescence signal was observed upon hybridization of the conjugates with the complementary sequence. When linked to the 5′-end of the ODNs, decreased changes were observed in all cases. When attached at the internal position of the ODN, there was either an increase or a decrease in the signal, depending on the cyanine and isomer used. Altogether, these results not only provide useful information on the preparation of ODN–cyanine conjugates involving the four nucleic bases but they also confirm the importance of the structural parameters in the design of fluorescent ODN probes.

Experimental Section

General methods: All solvents used were of the highest purity and did not contain more than 10 ppm H_2O. All chemicals were used as obtained unless otherwise stated. Cystamine dihydrochloride, 3-methylbenzothiazole-2-thione, 2-methylbenzothiazole, methyl iodide, lepidine, quinoline, quinaldine, 2-chloroquinoline, 4-chloroquinoline, 1,8-diiodooctane, acetic anhydride, pivaloyl chloride, tris(2-carboxyethyl)phosphane, and dioxane were purchased from Aldrich. Triethylamine and sodium sulfate were purchased from Merck, pyridine and dichloromethane from SDS, and acetonitrile and methanol from Labo-Standa. Analytical TLC was performed on precoated alumina plates (Merck silica gel 60F 254, ref. 5554), and preparative TLC on glass-backed silica plates (60F 254, ref. 5717). For flash chromatography, Merck silica gel 60 (70–230 mesh, ref. 7734) was used. Cyanine-containing compounds were directly visualized on the plates as colored spots. MM2 calculations were performed with Chem 3D Ultra 8.0.3 (Cambridge Soft Corporation). ODN syntheses were performed on an Expedite Nucleic Acid Synthesis system 8909 from Perseptive Biosystems. Reversed-phase chromatography was performed on a 600E (System Controller) equipped with a photodiode array detector (Waters 990) using a Lichrospher 100 RP 18 (5 μm) column (125 mm × 4 mm) from Merck with a linear gradient of CH_3CN in 0.1 M aqueous triethylammonium acetate, pH 7, with a flow rate of 1 mL min^{-1}. Mass-analysis ion-molecular weights of the ODNs were obtained by electrospray mass spectroscopy on a Quattro II (Micromas) instrument. ^{1}H and ^{13}C NMR spectra were recorded on a Varian Unity 500 Spectrometer. Absorption spectra were recorded with a Uvikon 860 spectrophotometer. Samples of cyanines **9**–**17** were prepared at a concentration of 1×10^{-6} M in MeOH. Fluorescence excitation and emission spectra were recorded on a Fluoromax 2 (ISA-Jobin-Yvon) spectrofluorimeter in 0.5 cm path length Suprasil quartz cuvettes (Hellma) with slits set at 0.5 mm (band pass = 2 nm). The spectra were corrected for the different output of the excitation lamp at the different wavelengths used for the experiment. To avoid inner filter effects and light reabsorption, solutions with maximal absorbance at the excitation wavelength of less than 0.1 were used.

Synthesis of cyanine-linker derivatives 9–17 (Scheme 1 and Table 1)

Synthesis of *N*-(8-iodooctyl)-2-methylbenzothiazolium iodide (7a): A mixture of 1,8-diiodooctane (1 mL, 1.85 g, 4.79 mmol) and 2-methylbenzothiazole (130 μL, 152 mg, 1 mmol) was heated at 150 °C. The reaction, monitored by TLC (CH_2Cl_2/MeOH 90/10), was stopped when the bis-alkylated product (R_f = 0.10) exceeded the mono-alkylated product (R_f = 0.32). After cooling to 0 °C, the obtained red oil was purified on a silica column with a gradient of MeOH (0 to 8 %) in CH_2Cl_2. After evaporation of the solvents, the residue was washed with cyclohexane and dried to give a light gray powder (164 mg, 32 %). ^{1}H NMR (500 MHz, [D$_6$]DMSO): δ = 8.43 (d, J = 9.6 Hz, 1H; H$_{Ar}$), 8.33 (d, J = 9.6 Hz, 1H; H$_{Ar}$), 7.88 (t, J = 9.6 Hz, 1H; H$_{Ar}$), 7.80 (t, J = 9.0 Hz, 1H; H$_{Ar}$), 4.69 (t, J = 8.4 Hz, 2H; N$^+$CH$_2$), 3.25 (t, J = 8.4 Hz, 2H; CH$_2$I), 3.20 (s, 3H; CH$_3$), 1.83 (q, J = 7.8 Hz, 2H; CH$_2$N$^+$), 1.73 (q, J = 7.8 Hz, 2H; CH$_2$), 1.42 (q, J = 7.8 Hz, 2H; CH$_2$), 1.22–1.36 ppm (m, 6H; CH$_2$); ESI-MS: m/z calcd for $C_{16}H_{23}INS$: 388.2, found: 388.2 [M+H$^+$].

Synthesis of 2-methylthio-3-methylbenzothiazolium iodide (8a): The synthesis was performed as previously reported.[51]

Synthesis of 3-(8-iodooctyl)-2-[(2,3-dihydro-3-methylbenzothiazol-2-ylidene)methyl]benzothiazolium iodide (9): A mixture of **7a** (96.9 mg, 188 μmol), **8a** (62.6 mg, 194 μmol), 1,2-dichloroethane (2 mL), and triethylamine (TEA) (8 μL, 57 μmol) was agitated to produce a dark yellow solution. After 2 h, the crude mixture was concentrated and purified on a silica column (CH_2Cl_2/MeOH 95/5) to give a dark yellow powder (60 mg, 47 %). R_f = 0.48 (CH_2Cl_2/MeOH 90/10). ^{1}H NMR (500 MHz, $CDCl_3$, TMS): δ = 7.91 (t, J = 10.8 Hz, 1H; H$_{Ar}$), 7.50 (m, 1H; H$_{Ar}$), 7.36 (m, 1H; H$_{Ar}$), 7.08 (s, 1H; −CH=), 4.91 (t, J = 7.84 Hz, 2H; N$^+$CH$_2$), 4.29 (s, 3H; CH$_3$N$^+$), 3.14 (t, J = 7.8 Hz, 2H; CH$_2$I), 1.90 (q, J = 7.8 Hz, 2H; CH$_2$CN$^+$), 1.75 (q, J = 7.8 Hz, 2H; CH$_2$I), 1.26 ~ 1.36 ppm (m, 8H; CH$_2$); ^{13}C NMR (500 MHz, $CDCl_3$): δ = 162.48, 161.99, 140.76, 140.49, 128.73, 128.70, 125.55, 125.37, 125.19, 125.14, 123.35, 123.22, 113.26, 113.07, 84.58, 48.53, 37.30, 33.53, 30.43, 29.42, 28.38, 27.71, 26.96, 7.66 ppm; ESI-MS: m/z calcd for $C_{24}H_{28}IN_2S_2$: 535.5, found: 535.1 [M+H$^+$]; UV/Vis (MeOH): $\lambda_{max}(\varepsilon)$ = 423 nm (85200 mol^{-1} cm^{-1}).

Synthesis of *N*-methyl-2-iodoquinolinium iodide (8b): A mixture of 2-chloroquinoline (200 mg, 1.22 mmol), dry CH_3CN (3 mL), and MeI (0.37 mL, 6.1 mmol) was heated at 55 °C in a sealed vial. After 10 h, TLC analysis (CH_2Cl_2/MeOH 90/10) indicated the formation of a new dark yellow product (R_f = 0.18). The mixture was concentrated and the residue washed with ethyl acetate (3 × 3 mL) to remove unconsumed 2-chloroquinoline, then **8c** was extracted with CH_2Cl_2 (3 × 3 mL). The solution was concentrated to give a dark yellow solid, used in the next synthesis step without any further purification (197 mg, 60 %). ESI-MS: m/z calcd for $C_{10}H_9ClN$: 178.6, found: 269.7 [M+H$^+$]. This corresponds to exchange of the chlorine atom by an iodine atom.

Synthesis of 3-(8-iodooctyl)-2-[(1,2-dihydro-1-methylquinolin-2-ylidene)-methyl]benzothiazolium iodide (10): A mixture of **7a** (91.5 mg, 178 μmol), **8b** (71.4 mg, 180 μmol), 1,2-dichloroethane(1 mL), MeOH (1 mL), and TEA (136 μL, 990 μmol) was agitated to produce a dark orange solution. After 24 h, the crude mixture was concentrated and purified on a silica column with a gradient of MeOH in CH_2Cl_2 (0 to 2 %) and then on preparative TLC plates (CH_2Cl_2/acetone/MeOH 75/22/3) to give an orange powder (93 mg, 80 %). ^{1}H NMR (500 MHz, $CDCl_3$, TMS): δ = 8.07 (t, J = 10.8 Hz, 1H; H$_{Ar}$), 8.05 (t, J = 10.8 Hz, 1H; H$_{Ar}$), 7.84 (d, J = 8.4 Hz, 1H; H$_{Ar}$), 7.80 (d, J = 8.4 Hz, 1H; H$_{Ar}$), 7.74 (d, J = 8.4 Hz, 1H; H$_{Ar}$), 7.68 (d, J = 8.4 Hz, 1H; H$_{Ar}$), 7.51 (t, J = 8.7 Hz, 1H; H$_{Ar}$), 7.48 (t, 1H; H$_{Ar}$), 7.34 (m, 2H; H$_{Ar}$), 6.53 (s, 1H; =CH−), 4.74 (t, J = 8.4 Hz, 2H; CH$_2$N$^+$), 4.42 (s, 3H; N$^+$CH$_3$), 3.15 (t, J = 8.4 Hz, 2H; CH$_2$I), 1.93 (q, J = 10.8 Hz, 2H; H$_{Ar}$), 1.77 (q, J = 8.4 Hz, 2H; H$_{Ar}$), 1.20–1.68 ppm (m, J = 10.8 Hz, 8H; H$_{Ar}$); ^{13}C NMR (500 MHz, $CDCl_3$, TMS): δ = 161.21, 154.39, 140.59, 140.24, 139.46, 133.64, 129.34, 128.30, 125.91, 125.08, 124.38, 123.82, 122.46, 118.98, 117.07, 112.67, 87.77, 48.03, 40.90, 33.42, 30.34, 29.32, 28.30, 27.45, 26.93, 7.60 ppm; ESI-MS: m/z calcd for $C_{26}H_{30}IN_2S$: 529.5, found: 529.1 [M+H$^+$]; UV/Vis (MeOH): $\lambda_{max}(\varepsilon)$ = 482 nm (38600 mol^{-1} cm^{-1}).

Synthesis of *N*-methyl-4-chloroquinolinium iodide (8c): Starting from 4-chloroquinoline compound **8c** was obtained as reported for the preparation of **8b**. The iodinated derivative was obtained as a byproduct. ESI-MS: m/z calcd for $C_{10}H_9ClN$: 178.6, found: 177.9 [M+H$^+$] (65 %), 269.9 ($C_{10}H_9IN$, 35 %).

Synthesis of 3-(8-iodooctyl)-2-[(1,4-dihydro-1-methylquinolin-4-ylidene)-methyl]benzothiazolium iodide (11): A mixture of **7a** (50 mg, 97 μmol), **8c** (33.5 mg, 97 μmol), 1,2-dichloroethane (1 mL), MeOH (1 mL), and TEA (68 μL, 495 μmol) was agitated to produce a dark red solution. After 4 h, the crude mixture was concentrated and purified on a silica column (CH_2Cl_2/MeOH 97.5/2.5) and then on preparative TLC plates (CH_2Cl_2/acetone/MeOH 75/22/3) to give a red powder (40 mg, 30 %). ^{1}H NMR (500 MHz, $CDCl_3$, TMS): δ = 8.73 (d, J = 10.8 Hz, 1H; H$_{Ar}$), 8.61 (d, J = 8.4 Hz, 1H; H$_{Ar}$), 8.05 (m, 3H; H$_{Ar}$), 7.76 (d, J = 9.0 Hz, 2H; H$_{Ar}$), 7.60 (t, J = 8.7 Hz, 1H; H$_{Ar}$), 7.40 (m, 2H; H$_{Ar}$), 6.94 (s, 1H; =CH−), 4.63 (t, J = 8.4 Hz, 2H; CH$_2$N$^+$), 4.17 (s, 3H; N$^+$CH$_3$), 3.19 (t, J = 8.4 Hz, 2H; CH$_2$I), 1.79 (q, J = 10.8 Hz, 2H; CH$_2$), 1.66 (q, J = 8.4 Hz, 2H; CH$_2$), 1.44 (m, 2H; CH$_2$), 1.21–1.34 ppm (m, 6H; CH$_2$); ^{13}C NMR (500 MHz, $CDCl_3$, TMS): δ = 159.73, 149.26, 145.65, 140.05, 138.22,

133.20, 128.29, 127.48, 125.91, 124.83, 124.76, 124.57, 122.88, 117.17, 112.20, 109.29, 88.06, 47.36, 43.10, 33.44, 30.43, 29.35, 28.41, 27.56, 27.07, 7.46 ppm; ESI-MS: m/z calcd for $C_{26}H_{30}IN_2S$: 529.5, found: 529.1 [M+H$^+$]; UV/Vis (MeOH): λ_{max} (ε) = 503 nm (58900 mol^{-1} cm^{-1}).

Synthesis of *N*-(8-iodooctyl)quinaldinium iodide 7b: A solution of diiodooctane (2.33 mL, 11.7 mmol) in dry dioxane (6 mL) was heated to 80 °C, and quinaldine (315 μL, 2.33 mmol) was added slowly over 45 min producing a brown solution. After 5 h, the solution was concentrated, and pentane (20 mL) added to give a black solid, which was collected by filtration, washed with pentane several times, and purified on a silica gel column with a MeOH gradient (0 to 4%) in CH_2Cl_2 to give a brown solid (120 mg, 10%). ^{1}H NMR (500 MHz, $CDCl_3$, TMS): δ = 9.01 (d, J = 8.5 Hz, 1H; H_{Ar}), 8.39 (d, J = 9.0 Hz, 1H; H_{Ar}), 8.31 (d, J = 8 Hz, 1H; H_{Ar}), 8.19 (t, J = 8 Hz, 1H; H_{Ar}), 8.13 (d, J = 8.25 Hz, 1H; H_{Ar}), 7.90 (d, J = 7.5 Hz, 1H; H_{Ar}), 5.08 (t, J = 8.4 Hz, 2H; CH_2N), 3.34 (s, 3H; N$^+$$CH_3$), 3.18 (t, J = 7.0 Hz, 2H; CH_2I), 2.0 (q, J = 8.0 Hz, 2H; CH_2), 1.80 (q, J = 7.0 Hz, 2H; CH_2I), 1.65 (q, 2H; J = 7.5 Hz, CH_2), 1.47–1.33 ppm (m, 6H; 3CH_2); ESI-MS: m/z calcd for $C_{18}H_{25}IN$: 382.3, found: 382.1 [M+H$^+$].

Synthesis of 1-(8-iodooctyl)-2-[(2,3-dihydro-3-methylbenzothiazol-2-ylidene)methyl]quinolinium iodide (12): A mixture of **8a** (29 mg, 90 μmol), **7b** (40 mg, 79 μmol), CH_2Cl_2 (1 mL), MeOH (1 mL), and TEA (24 μL, 170 μmol) was agitated to produce a dark orange solution. After 24 h, the mixture was concentrated and purified on a silica column with a MeOH gradient (0 to 3%) in CH_2Cl_2 and then on preparative TLC plates (CH_2Cl_2/acetone/MeOH 75/22/3) to give an orange powder (18.5 mg, 36%). ^{1}H NMR (500 MHz, $CDCl_3$, TMS): δ = 8.11 (d, J = 9.5 Hz, 1H; H_{Ar}), 8.00 (d, J = 9.0 Hz, 1H; H_{Ar}), 7.78 (m, 3H; H_{Ar}), 7.69 (d, J = 8.0 Hz, 1H; H_{Ar}), 7. 52 (t, J = 8 Hz, 1H; H_{Ar}), 7.50 (t, J = 7.5 Hz, 1H; H_{Ar}), 7.45 (d, J = 8.5 Hz, 1H; H_{Ar}), 7.34 (t, J = 8.0 Hz, 1H; H_{Ar}), 6.34 (s, 1H; =CH), 4.18 (s, 3H; N$^+$$CH_3$), 3.77 (t, J = 7.5 Hz, 2H; CH_2N), 3.18 (t, J = 7.0 Hz, 2H; CH_2I), 1.98 (m, 2H; CH_2), 1.80 (q, J = 7.0 Hz, 2H; CH_2), 1.45–1.65 ppm (m, 8H; 4CH_2); ^{13}C NMR (500 MHz,$CDCl_3$): δ = 162.37, 152.87, 140.86, 140.00, 139.45, 133.76, 129.94, 128.47, 125.96, 125.24, 124.69, 123.88, 122.58, 119.15, 116.57, 112.86, 86.90, 50.16, 36.58, 33.56, 30.49, 29.51, 28.49, 27.51, 27.00, 7.77 ppm; ESI-MS calcd for $C_{26}H_{30}IN_2S$: 529.5, found: 529.1 [M+H$^+$]; UV/Vis (MeOH): λ_{max}(ε) = 484 nm (69400 mol^{-1} cm^{-1}).

Synthesis of 1-(8-iodooctyl)-2-[(1,2-dihydro-1-methylquinolin-2-ylidene)-methyl]quinolinium iodide (13): A mixture of **8b** (71 mg, 180 μmol), **7b** (91 mg, 147 μmol), CH_2Cl_2 (1 mL), MeOH (1 mL), and TEA (140 μL, 1 mmol) was agitated to produce a dark red solution. After 24 h, the mixture was concentrated and purified on a silica column with a MeOH gradient (0 to 2%) in CH_2Cl_2 to give an oil, which was further purified on a preparative TLC plate with CH_2Cl_2/MeOH (99/1, 3×), CH_2Cl_2/MeOH (98/2, 2×), and CH_2Cl_2/MeOH (96/42×) to give a purple-red paste (18 mg, 19%). ^{1}H NMR (500 MHz, $CDCl_3$, TMS): δ = 7.40~7.95 (m, 12H; H_{Ar}), 5.85 (s, 1H; CH), 4.58 (m, 2H; CH_2N), 4.21 (s, 3H; NCH_3), 3.18 (t, J = 7.0 Hz, 2H; CH_2I), 1.96 (q, J = 7.5 Hz, 2H; NCH_2CH_2), 1.81 (q, J = 7.0 Hz, 2H; CH_2CH_2I), 1.20–1.40 ppm (m, 8H; 4CH_2); ^{13}C NMR (500 MHz, $CDCl_3$): δ = 154.91, 153.11, 140.26, 139.24, 138.70, 138.55, 132.94, 129.64, 129.20, 125.44, 125.28, 125.02, 124.88, 121.83, 121.64, 116.76, 115.93, 91.28, 49.79, 39.96, 33.37, 30.28, 29.19, 28.35, 27.22, 26.80, 7.63 ppm; ESI-MS: m/z calcd for $C_{28}H_{32}IN_2$: 523.5, found: 523.1 [M+H$^+$]; UV/Vis (MeOH): λ_{max}(ε) = 522 nm (69900 mol^{-1} cm^{-1}).

Synthesis of 1-(8-iodooctyl)-2-[(1,4-dihydro-1-methylquinolin-4-ylidene)-methyl]quinolinium iodide (14): A mixture of **8c** (29 mg, 85 μmol), **7b** (40 mg, 79 μmol), CH_2Cl_2 (1 mL), MeOH (1 mL), and TEA (23 μL, 170 μmol) was agitated to produce a dark purple solution. After 24 h, the crude mixture was concentrated and purified on a silica column using a MeOH gradient (0 to 3%) in CH_2Cl_2 to give a purple paste (21 mg, 45%). ^{1}H NMR (500 MHz, $CDCl_3$, TMS): δ = 8.68 (d, J = 7.5 Hz, 1H; H_{Ar}), 8.15 (d, J = 8.5 Hz, 1H; H_{Ar}), 8.06 (d, J = 9.5 Hz, 1H; H_{Ar}), 7.87 (d, J = 9.0 Hz, 1H; H_{Ar}), 7.84 (t, J = 7.5 Hz, 1H; H_{Ar}), 7.70 (m, 4H; H_{Ar}), 7.61 (m, 1H; H_{Ar}), 7.53 (d, J = 9.0 Hz, 1H; H_{Ar}), 7.40 (t, J = 7.5 Hz, 1H; H_{Ar}), 6.14 (s, 1H; =CH−), 4.34 (t, J = 7.5 Hz, CH_2N), 4.20 (s, 3H; NCH_3), 3.53 (t, J =7,0 Hz, 2H; CH_2), 3.18 (t, J =7,0 Hz, 2H; CH_2I), 1.40~1.60 ppm (m, 10H; CH_2); ^{13}C NMR (500 MHz,$CDCl_3$): δ = 153.76, 151.04, 144.98, 139.84, 139.26, 138.42, 133.50, 132.98, 129.89, 127.04, 125.63, 125.54, 125.48, 125.44, 122.23, 117.60, 115.91, 110.39, 92.72, 49.80, 43.08, 33.68, 30.68, 29.52, 28.80, 27.48, 27.22, 7.61 ppm; ESI-MS: m/z calcd for $C_{28}H_{32}IN_2$: 523.5, found: 523.1 [M+H$^+$]; UV/Vis (MeOH): λ_{max}(ε) = 557 nm (97000 mol^{-1} cm^{-1}).

Synthesis of 1-(8-iodooctyl)-4-[(2,3-dihydro-3-methylbenzothiazol-2-ylidene)methyl]quinolinium iodide (15): The synthesis was performed as previously reported for **8a** and **7c.**[70] ^{13}C NMR (500 MHz,$CDCl_3$): δ = 160.02, 149.07, 144.83, 140.28, 137.05, 132.99, 128.27, 127.27, 126.95, 124.80, 124.69, 124.54, 122.64, 116.78, 112.14, 109.25, 88.70, 55.10, 35.61, 33.51, 30.43, 29.50, 29.11, 28.42, 26.62, 7.54; ESI-MS: m/z calcd for $C_{26}H_{30}IN_2S$: 529.5, found: 529 [M+H$^+$]; UV/Vis (MeOH): λ_{max}(ε) = 503 nm (86400 mol^{-1} cm^{-1}).

Synthesis of 1-(8-iodooctyl)-4-[(1,2-dihydro-1-methylquinolin-2-ylidene)-methyl]quinolinium iodide (16): A mixture of **8b** (71 mg, 180 μmol), **7c** (90 mg, 172 μmol CH_2Cl_2 (1 mL), MeOH (1 mL), and TEA (140 μL, 1 mol) was agitated to produce a dark purple solution. After 24 h, the mixture was concentrated and purified on a silica column with a MeOH gradient (0 to 2%) in CH_2Cl_2 to give a purple paste (43 mg, 38%). ^{1}H NMR (500 MHz, $CDCl_3$, TMS): δ = 8.65 (d, J = 7.5 Hz, 1H; H_{Ar}), 8.34 (d, J = 8.5 Hz, 1H; H_{Ar}), 8.02 (d, J = 10.0 Hz, 1H; H_{Ar}), 7.87(d, J=9.0 Hz, 1H; H_{Ar}), 7.79 (t, J = 7.7 Hz, 1H; H_{Ar}), 7.67 (m, 4H; H_{Ar}), 7.59 (m, 2H; H_{Ar}), 7.40 (t, J = 7.5 Hz, 1H; H_{Ar}), 6.24 (s, 1H; =CH−), 4.51(t, J=7.5 Hz, 2H; CH_2N), 4.02 (s, 3H; N$^+$$CH_3$), 3.17 (t, J = 7.0 Hz, 2H; CH_2I), 1.94 (q, J = 7.5 Hz, 2H; NCH_2CH_2), 1.79 (q, J = 7.0 Hz, 2H; CH_2CH_2I), 1.20–1.60 ppm (m, 8H; 4CH_2); ^{13}C NMR (500 MHz, $CDCl_3$): δ = 154.55, 150.32, 143.77, 140.53, 137.87, 137.77, 133.06, 132.67, 129.21, 126.71, 126.66, 125.32, 125.25, 125.00, 122.12, 116.89, 116.34, 110.14, 94.77, 54.82, 39.14, 33.52, 30.45, 29.46, 29.15, 28.43, 26.68, 7.60 ppm; ESI-MS calcd for $C_{28}H_{32}IN_2$: 523.5, found: 523.1 [M+H$^+$]; UV/Vis (MeOH): λ_{max}(ε) = 556 nm (98000 mol^{-1} cm^{-1}).

Synthesis of 1-(8-iodooctyl)-4-[(1,4-dihydro-1-methylquinolin-4-ylidene)-methyl]quinolinium iodide (17): A mixture of **7c** (100 mg, 196 μmol), **8c** (67 mg, 200 μmol), CH_2Cl_2 (1 mL), MeOH (1 mL), and TEA (25.3 μL, 1.1 mmol) was agitated to produce a dark blue solution. After 24 h, the mixture was concentrated and purified on a silica column (CH_2Cl_2/MeOH 98/2) to give an intensely blue paste (35 mg, 39%). ^{1}H NMR (500 MHz, $CDCl_3$, TMS): δ = 7.51~8.34 (m, 12H; H_{Ar}), 7.03 (s, 1H; CH), 4.36 (t, J =7,5 Hz, 2H; CH_2N), 4.07 (s, 3H; NCH_3), 3.16 (t, J = 7.0 Hz, 2H; CH_2I), 1.92 (q, J = 7.5 Hz, 2H; NCH_2CH_2), 1.78 (q, J = 7.0 Hz, 2H; CH_2CH_2I), 1.20–1.40 ppm (m, 8H 4CH_2); ^{13}C NMR (500 MHz,$CDCl_3$) δ = 149.43, 149.35, 143.31, 142.62, 138.69, 137.76, 132.68, 132.58, 126.30, 126.14, 125.77, 125.48, 125.41, 116.83, 116.76, 109.87, 109.73, 97.22, 54.61, 42.58, 33.34, 30.26, 29.18, 28.96, 28.25, 26.53, 7.43 ppm. ESI-MS: m/z calcd for $C_{28}H_{32}IN_2$: 523.5, found: 523.2 [M+H$^+$]; UV/Vis (MeOH): λ_{max}(ε) = 589 nm (70470 mol^{-1} cm^{-1}).

Synthesis of the ODN–cyanines conjugates (Scheme 2)

Synthesis of oligonucleotides 4 and 5: The ODNs were assembled by classical phosphoramidite chemistry on a controlled pore glass (CPG) support on a micromole scale. After drying of the supports bearing the ODNs with a free 5′-hydroxyl group (1 μmol), *O*-(6-dimethoxytrityloxy-3,4-dithiahexyl-H-phosphonate (0.025 g, 0.04 mmol) in pyridine/CH_3CN (50/50, 0.4 mL, dried overnight on 3 and 4 Å molecular sieves) and a solution of pivaloyl chloride (0.020 g, 0.166 mmol) in CH_3CN (0.5 mL, prepared 1 h before use and dried over 3 Å molecular sieves) were added simultaneously to the ODN chain bound to the support. After 2.5 min, the solution was removed, and the support washed with anhydrous pyridine/CH_3CN (50/50, 3×1 mL). Then a sulfur solution (50 mg S_8 in a CS_2/pyridine (2.5 mL, 3/2)) was added. After 20 min, the solution was removed, and the support washed with pyridine/CH_3CN (50/50, 3×1 mL) and then with acetonitrile (3×1 mL). ODNs **4** and **5** were deprotected and cleaved from the support by treatment with concentrated aqueous ammonia for 6 h at 50 °C. After removal of the ammonia solution, the crude ODNs **4** and **5** were analyzed by reversed-phase chromatography with a linear gradient of CH_3CN (0 to 24% in 30 min). Detection λ = 260 nm. R_t(**4**) = 19 min, 26 s. R_t(**5**) = 14 min, 16 s.

Synthesis of conjugates 4 and 5: Before conjugate synthesis, MeOH was passed over Chelex resin 100 to remove divalent ions. Methanolic

solutions of the cyanine-linker derivatives (1.5 mg in 400 μL) were added to vortexed solutions of **4** or **5** (10 opitical density (OD) each) in MeOH (400 μL) containing [18]crown-6 (10 mg). After 17 h, the coupling efficiency was checked by reversed-phase chromatography with a linear gradient of CH_3CN (16 to 40% over 30 min). ODN–cyanine conjugates were obtained with longer retention times as compared to the starting ODN–linker derivatives **4** and **5**. During the entire workup, ODN mixtures were maintained below 50°C and protected from light. The crude mixture was evaporated to dryness and solubilized with a 1 M NaH_2PO_4 solution containing 10% MeOH (2 mL). Excess dye was extracted with CH_2Cl_2 (3×3 mL). The aqueous phase was passed through a Sephadex G25 column, and the fast-eluting colored fractions collected and purified by reversed-phase chromatography under the conditions described above. (See Table 1 for retention times and mass-analysis data.) Yields: $\mathbf{4}_{\mathbf{Th}}$, $\mathbf{4}_{\mathbf{4TO}}$, $\mathbf{5}_{\mathbf{Th}}$, and $\mathbf{5}_{\mathbf{4TO}}$ (35–40%); $\mathbf{4}_{\mathbf{2TO'}}$, $\mathbf{4}_{\mathbf{4TO}}$, $\mathbf{5}_{\mathbf{2TO}}$, $\mathbf{5}_{\mathbf{2TO'}}$ (20–25%); and other conjugates involving the quinocyanines (10–13%).

Synthesis of ODN linker derivative 6: The ODN was assembled by classical phosphoramidite chemistry on a CPG support on a micromole scale, except that at the site selected for the introduction of the linker, a coupling step using H-phosphonate chemistry was manually performed as follows: N^6-Benzoyl-5′-*O*-(4,4′-dimethoxytrityl)-2′-deoxyadenosine-3′-H-phosphonate (0.033 g, 0.04 mmol) in pyridine/CH_3CN (50/50, 0.4 mL) and pivaloyl chloride (0.02 g, 0.166 mmol) in pyridine/CH_3CN (50/50, 0.5 mL) were added simultaneously to the detritylated ODN bound to the support. After 2.5 min, the solution was removed and the support washed with anhydrous pyridine/CH_3CN (50/50, 1 mL, 3×). Then cystamine (0.165 g, 0.87 mmol) in pyridine/CCl_4 (50/50, 1 mL) was added. After 1 h, the solution was removed and the support washed with anhydrous pyridine/CH_3CN (50/50, 1 mL, 3×) and then with anhydrous CH_3CN (1 mL, 3×). The support was treated with a mixture of capping solutions used on the synthesizer (0.5 mL each) for 10 min, washed with CH_3CN (1 mL, 4×), and dried. The ODN chain assembly was completed by phosporamidite chemistry to give the fully protected 14-mer ODN **6** bound to the support bearing the linker at its central phosphate. At the end of the chain assembly an additional detritylation step was performed to deblock the 5′-terminal hydroxyl function. The deprotection step was completed by treatment with concentrated aqueous ammonia overnight at 50°C. Reversed-phase chromatography was performed with a linear gradient of CH_3CN (8 to 28% over 25 min). Two roughly equivalent peaks with close retention times, R_t(**16a**) = 10 min 54 s and R_t(**16b**) = 11 min 45 s, corresponding to the isomers of ODN **6** were obtained and separated by using a linear gradient of CH_3CN (5 to 25% over 60 min).

Coupling reaction between each pure isomer of ODN 6 and cyanine-linker derivatives 9, 11, 15, and 17: Solutions of $\mathbf{6}_{R_P}$ and $\mathbf{6}_{S_P}$ (8 OD each) in a 0.5% aqueous bicarbonate buffer (pH 9, 400 μL) were degassed by a stream of argon. Then a tris(2-carboxyethyl)phosphine (TCEP) solution (20 mg in 300 μL water, 3 μL) was added. After 10 min, a DMF solution of a cyanine-linker derivative (1.5 mg in 400 μL) was added and vigorously vortexed. Another 3 μL of a TCEP solution was added. After overnight reaction, the coupling efficiency was checked by reversed-phase analysis under the same conditions as described above. Starting from each pure ODN linker isomer $\mathbf{6}_{R_P}$ and $\mathbf{6}_{S_P}$ ODN–cyanine conjugates were obtained with increased retention times as compared to the starting ODN-linker derivatives $\mathbf{6}_{R_P}$ and $\mathbf{6}_{S_P}$. During the entire workup, solutions of conjugates were maintained below 50°C and protected from light. Mixtures were evaporated to dryness by using xylene/DMF azeotrope. The residue was dissolved in a 1 M solution of NaCl in H_2O/MeOH (80/20, 2 mL) and extracted several times with CH_2Cl_2. The aqueous phase was passed over a size-exclusion Sephadex G 25 column with water as eluant. Fast-eluted colored fractions were purified by reversed-phase chromatography under the conditions described above (see Table 2 for retention times and mass-analysis data). Yields: $\mathbf{6}_{\mathbf{Th}R_P}$ and $\mathbf{6}_{\mathbf{Th}S_P}$ (20%), $\mathbf{6}_{\mathbf{4TO}R_P}$ and $\mathbf{6}_{\mathbf{4TO}S_P}$ (15%), $\mathbf{6}_{\mathbf{4TO'}R_P}$ and $\mathbf{6}_{\mathbf{4TO'}S_P}$ (13%), $\mathbf{6}_{\mathbf{44'Q}R_P}$ and $\mathbf{6}_{\mathbf{44'Q}S_P}$ (5 and 7%, respectively). Electrospray mass analysis confirmed the mass of conjugates $\mathbf{6}_{\mathbf{Th}S_P}$, $\mathbf{6}_{\mathbf{44'Q}R_P}$, and $\mathbf{6}_{\mathbf{44'Q}S_P}$, while for conjugates $\mathbf{6}_{\mathbf{Th}R_P}$, $\mathbf{6}_{\mathbf{4TO}R_P}$, $\mathbf{6}_{\mathbf{4TO}S_P}$, $\mathbf{6}_{\mathbf{4TO'}R_P}$, and $\mathbf{6}_{\mathbf{4TO'}S_P}$, masses 13–16 units higher were found.

Binding properties of the oligonucleotide–cyanine conjugates

Determination of the molar extinction coefficients: Concentrations of target ODN **3** and unmodified ODNs **1** and **2** were calculated from molar extinction coefficients at 260 nm determined by the nearest-neighbor model[74] (ODN **1**: $\varepsilon_{260} = 133\,600\ M^{-1}cm^{-1}$, ODN **2**: $\varepsilon_{260} = 115\,700\ M^{-1}cm^{-1}$, ODN **3**: $\varepsilon_{260} = 278\,900\ M^{-1}cm^{-1}$). The molar extinction coefficients ε for conjugates **4** were determined by titrating the conjugate solutions in a 10 mM sodium cacodylate buffer (pH 7) containing 100 mM NaCl at 5°C with a solution of single-stranded complementary sequence **3.** The changes in absorbance observed at 260 nm (corrected for dilution) on stepwise additions of small volumes (10 μL) of a conjugate **4** (ca. 1 μM based on the molar extinction coefficient values of cyanines **9**–**17**) were plotted versus the concentration of ODN **3**. The breaks observed in the titration curves correspond to the equivalence of concentrations for both ODN **3** and conjugate **4** considered. Because the concentration of ODN **3** was known, it was possible to determine the ε values of conjugates **4** by using the Lambert–Beer law.

T_m determination by absorption spectroscopy: All concentrations are given on a per-strand basis. For the melting studies, 1 μM ODN solutions (each strand) were used in a 10 mM sodium cacodylate buffer (pH 7) containing 100 mM NaCl. Duplex stabilities were determined by thermal denaturation.[61] The uncertainty in the T_m values was ±0.5°C.

Fluorescence studies: Fluorescence experiments (Table 4) were performed with the same concentrations of ODN conjugates or duplex and the same buffer conditions as used for the binding studies. The excitation wavelengths used for both the free conjugates and the corresponding duplexes were the λ_{max} of the excitation spectra recorded for each conjugate. The emission spectra of the free conjugates were recorded at 5°C (between $\lambda = 450$ and 700 nm). A small volume of target sequence **3** (1 equiv) was added, and the mixture allowed to hybridize in the dark at 5°C for 6 h to ensure complete hybridization. The emission spectra of the duplexes were corrected for the changes in absorbance observed on duplex formation.

Acknowledgements

We thank the CNRS and the Region Centre for a fellowship to R.L., C. Buré for running the electrospray mass spectrometer, and H. Meudal for recording the NMR spectra.

[1] International Human Genome Sequencing Consortium, *Nature* **2001**, *409*, 860–921 (248 authors).
[2] J. C. Venter, M. D. Adams, E. W. Myers, P. W. Li, R. J. Mural, G. G. Sutton, H. O. Smith, M. Yandell, C. A. Evans, R. A Holt and 273 others, *Science* **2001**, *291*, 1304–1351.
[3] N. J. Risch, *Nature* **2000**, *405*, 847–856.
[4] A. D. Roses, *Nature* **2000**, *405*, 857–865.
[5] F. S. Collins, E. D. Green, A. E. Guttmacher, M. S. Guyer, *Nature* **2003**, *422*, 835–847.
[6] B. W. Kirk, M. Feinsod, R. Favis, R. M. Kliman, F. Barany, *Nucleic Acids Res.* **2002**, *30*, 3295–3311.
[7] T. S. Tanaka, T. Kunath, W. L. Kimber, S. A. Jaradat, C. A. Stagg, M. Usuda, T. Yokota, H. Niwa, J. J. Rossant, M. S. H. Ko, *Genome Res.* **2002**, *12*, 1921–1928.
[8] M. Blow, P. A. Futreal, R. Wooster, M. R. Stratton, *Genome Res.* **2004**, *14*, 2379–2387.
[9] M. Niemeyer, D. Blohm, *Angew. Chem.* **1999**, *111*, 3039–3043; *Angew. Chem. Int. Ed.* **1999**, *38*, 2865–2869.
[10] M. S. Schchepinov, S. C. Case-Green, E. M. Southern, *Nucleic Acids Res.* **1997**, *25*, 1155–1161.
[11] L. Zhang, M. F. Miles, K. D. Aldape, *Nat. Biotechnol.* **2000**, *21*, 818–821.
[12] E. Morrison, *J. Fluorescence* **1999**, *9*, 187–196.
[13] R. M. Clegg, *Methods Enzymol.* **1992**, *211*, 353–388.
[14] S. Tyagi, F. R. Kramer, *Nat. Biotechnol.* **1996**, *17*, 303–308.
[15] A. Yamane, *Nucleic Acids Res.* **2002**, *30*, e97.

[16] R. A. Cardullo, S. Agrawal, C. Flores, P. C. Zamecnik, D. E. Wolf, *Proc. Natl. Acad. Sci. USA* **1988**, *85*, 8790–8794.
[17] J.-L. Mergny, A. S. Boutorine, T. Garestier, F. Belloc, M. Rougée, N. V. Bulychev, A. A. Koshkin, J. Bourson, A. V. Lebedev, B. Valeur, N. T. Thuong, C. Hélène, *Nucleic Acids Res.* **1994**, *22*, 920–928.
[18] P. R. Selvin, J. E. Hearst, *Proc. Natl. Acad. Sci. USA* **1994**, *91*, 10024–10028.
[19] K. Ebata, M. Masuko, H. Ohtani, M. Kashiwasake-Jibu, *Photochem. Photobiol.* **1995**, *62*, 836–839.
[20] P. L. Paris, J. M. Langenhan, E. T. Kool, *Nucleic Acids Res.* **1998**, *26*, 3789–3793.
[21] E. Kostenko, M. Dobrikov, D. Pyshnyi, V. Petyuk, N. Komarova, V. Vlassov, M. Zenkova, *Nucleic Acids Res.* **2001**, *29*, 3611–3620.
[22] F. D. Lewis, Y. Zhang, R. L. Letsinger, *J. Am. Chem. Soc.* **1997**, *119*, 5451–5452.
[23] K. Yamana, T. Iwai, Y. Ohtani, S. Sato, M. Nakamura, H. Nakano, *Bioconjugate Chem.* **2002**, *13*, 1266–1273.
[24] K. Wiederholt, S. B. Rajur, J. Giuliano, M. J. O'Donnell, L. W. McLaughlin, *J. Am. Chem. Soc.* **1996**, *118*, 7055–7062.
[25] S. B. Rajur, J. Robles, K. Wiederholt, R. G. Kuimelis, L. W. McLaughlin, *J. Org. Chem.* **1997**, *62*, 523–529.
[26] Y. Jenkins, J. K. Barton, *J. Am. Chem. Soc.* **1995**, *117*, 8736–8738.
[27] D. Garcia-Fressnadillo, N. Boutonnet, S. Schumm, C. Moucheron, A. Kirsch-De Mesmaeker, E. Defrancq, J. F. Constant, J. Lhomme, *Biophys. J.* **2002**, *82*, 978–987.
[28] G. N. Grimm, A. S. Boutorine, P. Lincoln, C. Hélène, B. Norden, *ChemBioChem* **2002**, *3*, 324–331.
[29] K. Yamana, H. Zako, K. Asazuma, R. Iwase, A. Nakatano, A. Murakami, *Angew. Chem.* **2001**, *113*, 1138–1140; *Angew. Chem. Int. Ed.* **2001**, *40*, 1104–1106.
[30] A. Okamoto, K. Kanatani, I. Saito, *J. Am. Chem. Soc.* **2004**, *126*, 4820–4827.
[31] Y. Saito, Y. Miyauchi, A. Okamoto, I. Saito, *Tetrahedron Lett.* **2004**, *45*, 7827–7831.
[32] T. Ishiguro, J. Saitoh, H. Yawata, M. Otsuka, T. Inoue, Y. Sugiura, *Nucleic Acids Res.* **1996**, *24*, 4992–4997.
[33] T. Inoue, Y. Sugiura, J. Saitoh, T. Ishiguro, M. Otsuka, *Bioorg. Med. Chem.* **1999**, *7*, 1207–1211.
[34] M. Kubista, N. Svanvik, CA 2451442A/1, **1997**; [*Chem. Abstr.* **1997**, *128*, 58278j].
[35] N. Svanvik, G. Westman, D. Wang, M. Kubista, *Anal. Biochem.* **2000**, *281*, 26–35.
[36] J. Isacsson, I. Cao, L. Ohlsson, S. Nordgren, N. Svanvik, G. Westman, M. Kubista, R. Sjöback, U. Sehlstedt, *Mol. Cell. Probes* **2000**, *14*, 321–328.
[37] N. Svanvik, J. Nygren, G. Westman, M. Kubista, *J. Am. Chem. Soc.* **2001**, *123*, 803–809.
[38] O. Seitz, F. Bergmann, D. Heindl, *Angew. Chem.* **1999**, *111*, 2340–2343; *Angew. Chem. Int. Ed.* **1999**, *38*, 2203–2206.
[39] O. Köhler, O. Seitz, *Chem. Commun.* **2003**, 2938–2939.
[40] O. Köhler, D. V. Jarikote, O. Seitz, *ChemBioChem* **2005**, *6*, 69–77.
[41] C. P. Linn, J. B. Pitner, EP 0710668A/2 **1996**; [*Chem. Abstr.* **1996**, *124*, 309549].
[42] E. Privat, U. Asseline, *Bioconjugate Chem.* **2001**, *12*, 757–769.
[43] E. Privat, T. Melvin, U. Asseline, P. Vigny, *J. Photochem. Photobiol. B* **2001**, *74*, 532–541.
[44] E. Privat, T. Melvin, F. Merola, G. Schweizer, S. Prodhomme, U. Asseline, P. Vigny, *Photochem. Photobiol.* **2002**, *75*, 201–210.
[45] U. J. Krull, *Anal. Chim. Acta* **2002**, *470*, 57–70.
[46] X. Wang, U. J. Krull, *Bioorg. Med. Chem. Lett.* **2005**, *15*, 1725–1729.
[47] L. G. S. Brooker, G. H. Keyes, *J. Am. Chem. Soc.* **1937**, *59*, 74–79.
[48] L. G. S. Brooker, G. H. Keyes, W. W. Williams, *J. Am. Chem. Soc.* **1942**, *64*, 199–210.
[49] G. de W. Anderson in *Chemistry of Carbon Compounds, Vol. 4b* (Ed: E. H. G.Rodd), Elsevier, Amsterdam, **1959**, pp. 1053–1080.
[50] A. Mishra, R. K. Behera, P. K. Behera, B. K. Mishra, G. B. Behera, *Chem. Rev.* **2000**, *100*, 1973–2011.
[51] H. S. Rye, S. Yue, D. E. Wemmer, M. A. Quesada, R. P. Haugland, R. A. Mathies, A. N. Glazer, *Nucleic Acids Res.* **1992**, *20*, 2803–2812.
[52] Z. Zeng, S. C. Benson, A. N. Glazer, *Anal. Biochem.* **1995**, *231*, 256–260.
[53] A. N. Glazer, H. S. Rye, *Nature* **1992**, *359*, 859–861.
[54] H. S. Rye, A. N. Glazer, *Nucleic Acids Res.* **1995**, *23*, 1215–1222.
[55] J. Nygren, N. Svanvik, M. Kubista, *Biopolymers* **1998**, *1*, 39–51.
[56] S. Prodhomme, J-P. Demaret, S. Vinogradov, U. Asseline, L. Morin-Allory, P. Vigny, *J. Photochem. Photobiol. B* **1999**, *53*, 60–69.
[57] L. G. Lee, C-H. Chen, L. A. Liu, *Cytometry* **1986**, *7*, 508–517.
[58] N. I. Gadjev, T. D. Deligeorgiev, S. H. Kim, *Dyes Pigm.* **1999**, 40, 181–186.
[59] T. D. Deligeorgiev, D. A. Zaneva, S. H. Kim, R. W. Sabnis, *Dyes Pigm.* **1998**, *37*, 205–211.
[60] A. Larsson, C. Carlsson, M. Jonsson, B. Albinsson, *J. Am. Chem. Soc.* **1994**, *116*, 8459–8465.
[61] U. Asseline, M. Delarue, G. Lancelot, F. Toulme, N. T. Thuong, T. Montenay-Garestier, C. Hélène, *Proc. Natl. Acad. Sci. USA* **1984**, *81*, 3297–3301.
[62] U. Asseline, N. T. Thuong, C. Helene, *New J. Chem.* **1997**, *21*, 5–17.
[63] N. T. Thuong, U. Asseline in *Current Protocols in Nucleic Acid Chemistry* (Eds: S. Beaucage, D. E. Bergstrom, G. D. Glick, R. A. Jones), Wiley, New York, **2001**, pp. 4.9.1–4.9.28.
[64] R. Lartia, U. Asseline, *Tetrahedron Lett.* **2004**, *45*, 5949–5952.
[65] U. Asseline, F. Toulme, N. T. Thuong, M. Delarue, T. Montenay-Garestier, C. Hélène, *EMBO J.* **1984**, *3*, 795–800.
[66] U. Asseline, E. Bonfils, D. Dupret, N. T. Thuong, *Bioconjugate Chem.* **1996**, *7*, 369–379.
[67] F. M. Hamer, *J. Chem. Soc.* **1928**, *127*, 206–214.
[68] J. Metzger, H. Larivé, R. Dennilauler, R. Baralle, C. Gaurat, *Bull. Soc. Chim. Fr.* **1967**, *1*, 57–65.
[69] U. Asseline, N. T. Thuong in *Current Protocols in Nucleic Acid Chemistry* (Eds: S. Beaucage, D. E. Bergstrom, G. D. Glick, R. A. Jones), Wiley, New York, **2001**, pp. 4.8.1–4.8.15.
[70] J. A. Fidanza, H. Ozaki, L. W. McLaughlin in *Methods in Molecular Biology, Vol. 26* (Ed: S. Agrawal), Humana press, Totowa, **1994**, pp. 121–173.
[71] J. A. Burns, J. C. Butler, J. Moran, G. M. Whitesides, *J. Org. Chem.* **1991**, *56*, 2648–2650.
[72] S. Chatuverdi, T. Horn, R. L. Letsinger, *Nucleic Acids Res.* **1996**, *24*, 2318–2323.
[73] U. Asseline, M. Chassignol, J. Draus, M. Durand, J.-C. Maurizot, *Bioorg. Med. Chem.* **2003**, *11*, 3499–3511.
[74] C. R. Cantor, R. Warshaw, M. M. Shapiro, *Biopolymers* **1970**, *9*, 1059–1077.
[75] L. K. Jensen, C. H. Gotfredsen, K. Bondensgaard, J. P. Jacobsen, *Acta Chem. Scand.* **1998**, *52*, 641–650.
[76] F. D. Lewis, R. L. Letsinger, M. R. Wasielewski, *Acc. Chem. Res.* **2001**, *34*, 159–170.
[77] T. L. Netzel, K. Nafisi, M. Zhao, J. R. Lenhard, I. Johnson, *J. Phys. Chem.* **1995**, *99*, 17936–17947.
[78] J. R. Carreon, K. P. Mahon, S. O. Kelly, *Org. Lett.* **2004**, *6*, 517–519.

Received: July 28, 2005
Revised: October 19, 2005
Published online: January 18, 2006

